Supporting Information

A cellphone-based colorimetric multi-channel sensor for water environmental monitoring

Yunpeng Xing[a,b1], Boyuan Xue[b1], Yongshu Lin[b], Xueqi Wu[a], Fang Fang[c], Peishi Qi[a*], Jinsong Guo[c*], Xiaohong Zhou[a*]

[a] State Key Laboratory of Urban Water Resource and Environment, School of Environment, Harbin Institute of Technology, Harbin 150090, China

[b] State Key Joint Laboratory of ESPC, Center for Sensor Technology of Environment and Health, School of Environment, Tsinghua University, Beijing 100084, China

[c] Key Laboratory of the Three Gorges Reservoir Region's Eco-Environments of MOE, Chongqing University, Chongqing 400030, China

* Corresponding author:

Peishi Qi, qipeishi@163.com; Jinsong Guo, guo0768@cqu.edu.cn; Xiaohong Zhou, xhzhou@mail.tsinghua.edu.cn

[1] These authors contributed equally to this work.

Summary

- Number of pages: 16

- Number of figures: 7

- Number of notes: 4

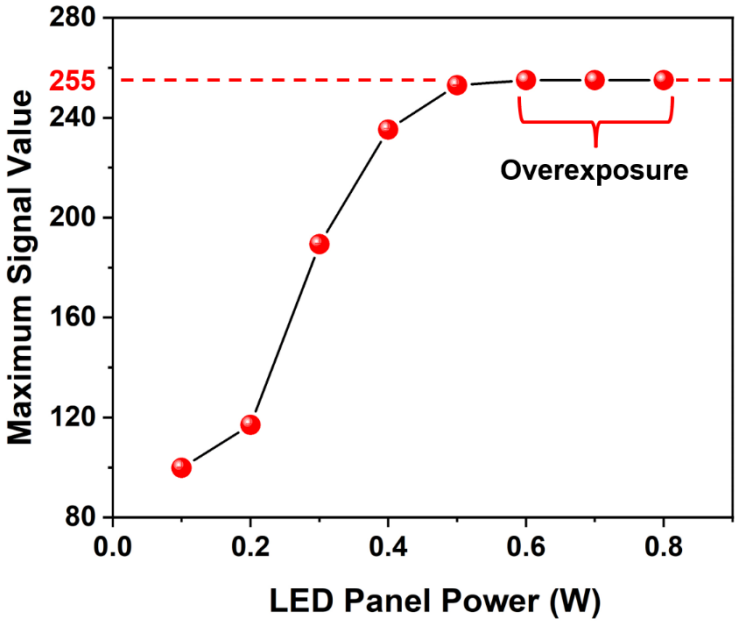

Fig. S1 The optimization of light source power (n=3). The horizontal axis is the power of LED panel, and the vertical axis is the maximum signal value (i.e. gray value) of the whole spectrum. When the power was above 0.5 W, overexposure happened and signal value reached its maximum 255.

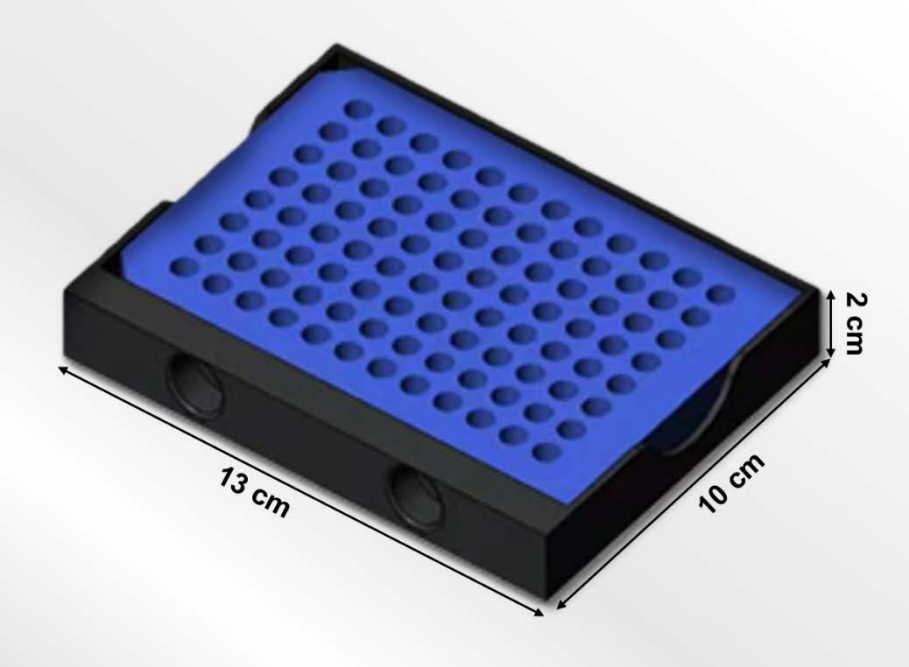

Fig. S2 The structural design of the 3D-printed plate. The plate was designed with walls between each channel and manufactured using Acrylonitrile Butadiene Styrene (ABS) plastic.

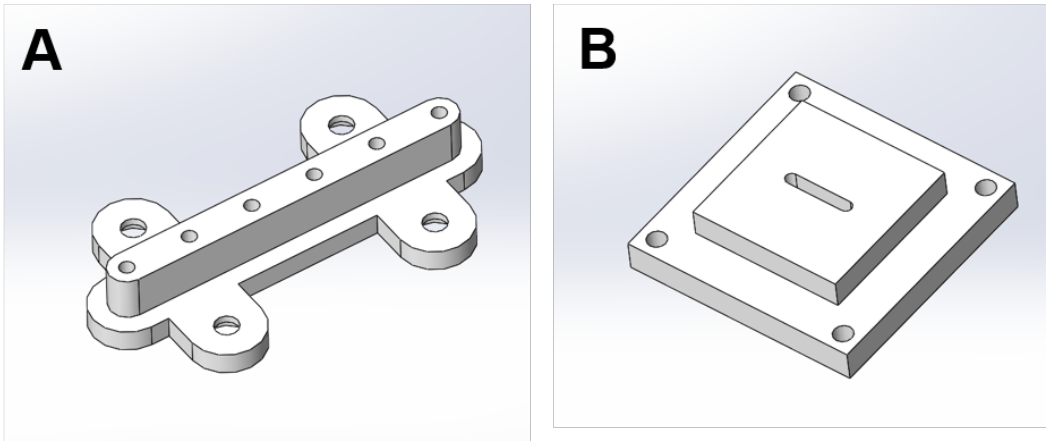

Fig. S3 The structural design of the optical fiber fixators. (A) The structure of the front optical fiber fixator; (B) The structure of the back optical fiber fixator. From the front end to the back end, the imaging geometry shrunk approximately four times.

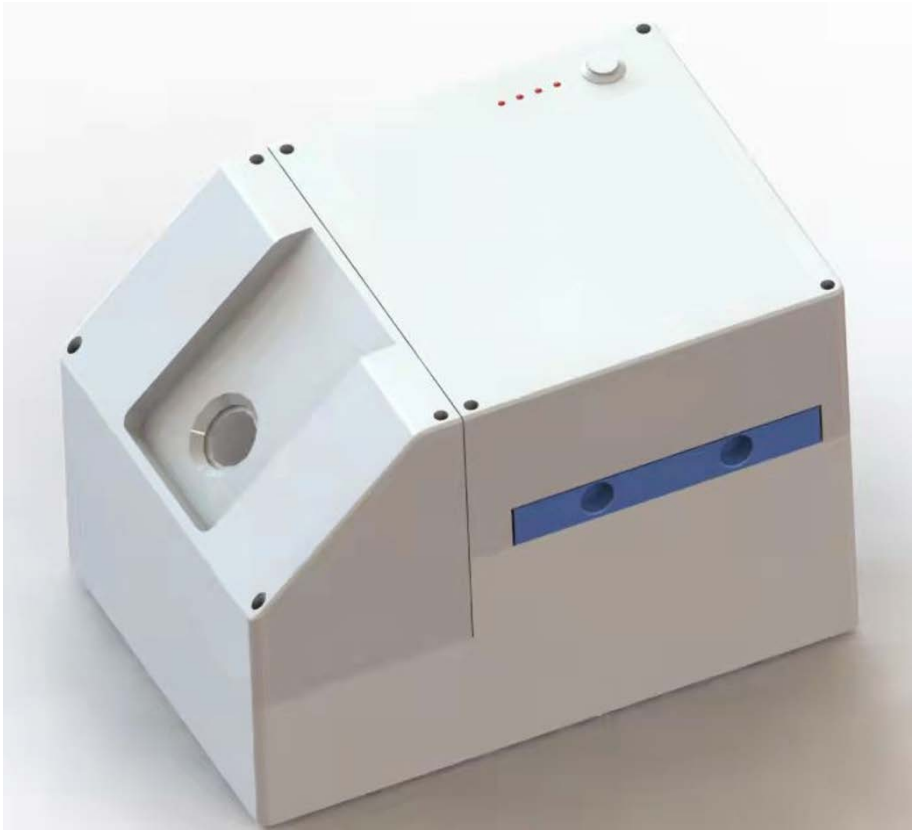

Fig. S4 The appearance dimension of the cellphone-based multi-channel sensor.

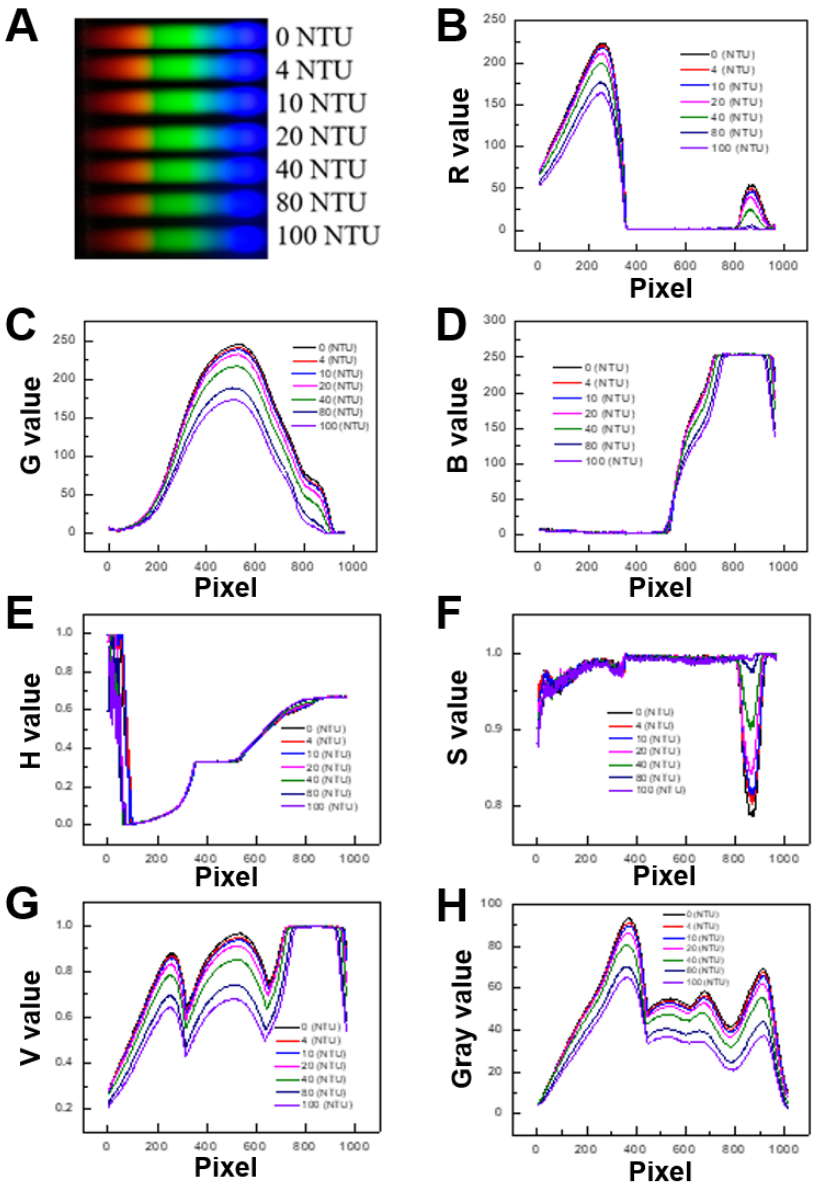

Fig. S5 Quantitative performance of different image analysis models. (A) Spectra of turbidity at different concentration; Spectral curves of model (B) R, (C) G, and (D) B; spectral curves of model (E) H, (F) S, and (G) V; Spectral curve of model (G) gray value.

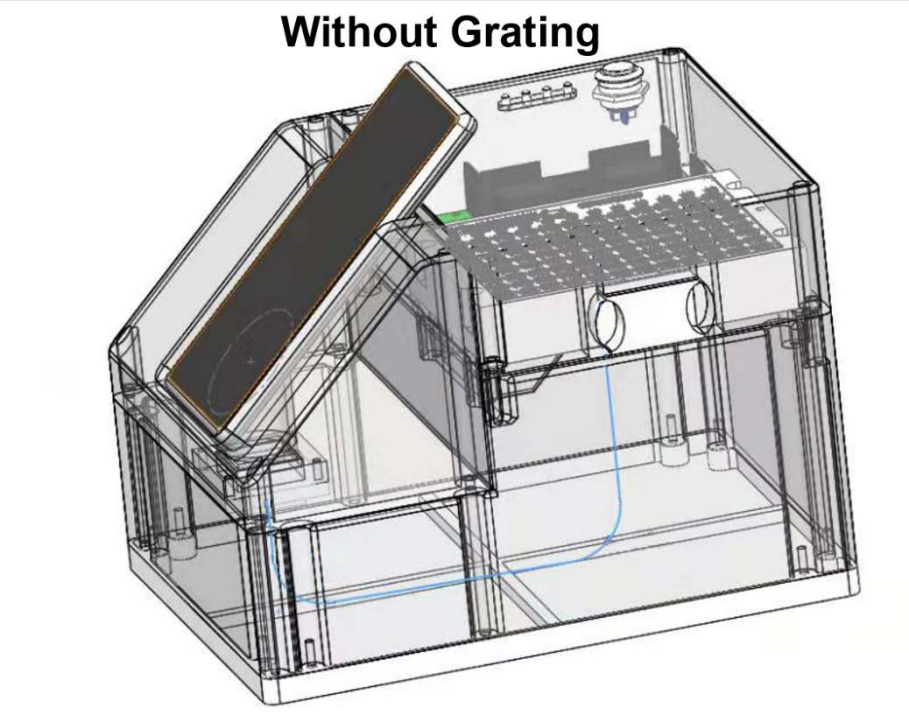

Fig. S6 The structural design of the cellphone-based multi-channel sensor without grating. The transmission light was directly captured by the CMOS camera of the cellphone without diffraction.

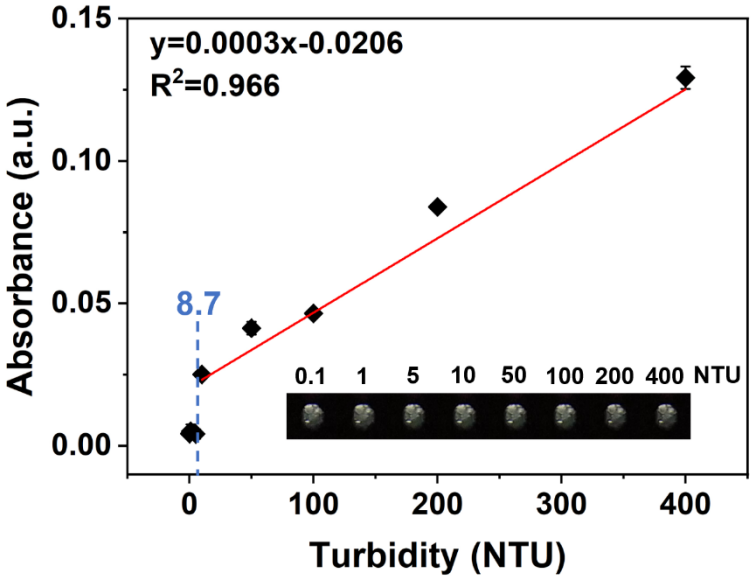

Fig. S7 The calibration curve for turbidity without grating (n=3). Under different turbidity, the average signal value (gray value) of the transmission light was directly calculated and the absorbance was similarly obtained by **Eq. 4**.

Note S1 The selection and determination of the grating.

The grating formula (**Eq. S1**) shows the relationship between the diffraction angle and the wavelength.

$$d(sin\alpha + sin\beta) = m\lambda \quad \text{(S1)}$$

where d is the interval distance of lines, α is the incident angle, β is the diffraction angle, m is the spectral series (m = 0, ±1, ±2…), and λ is the wavelength.

The more lines are ruled, the higher the spectral resolution, and the less lines are ruled, the wider the spectral coverage (**Eq. S1**). Therefore, the number of lines should be carefully determined to balance the spectral resolution and coverage. In our design, only one diffraction spectrum was needed for analysis, hence the number of lines should be set as large as possible. Considering the limit of ruling (<1500 lines/mm), 1200 lines/mm grating was finally chosen.

In addition, the blazing angle of the grating was 36.9°, i.e. the diffraction efficiency reached maximum when the diffraction angle was 36.9°. In our design, the blazing angle was at 500 nm wavelength of the first-order diffraction spectrum. Thus, to ensure the diffraction efficiency, the first-order diffraction spectrum with the strongest intensity was captured and analyzed, and the angle of grating was adjusted to eliminate the optical interference caused by the zero- and second-order diffraction spectrum.

Note S2 The image quantization codes in the process of establishing image analysis model.

A=cell(a_1,a_2)——Create a matrix of a_1 rows and a_2 columns;

for i=b_1:b_2——Create a for loop with start value b_1 and stop value b_2 (depending on the number of the image);

name=strcat('*name*',num2str(i),'.*JPG*')——Import image name;

A{i}=imread(name)——Read the image into matrix A;

[X,Y]=ginput(2)——Select two points to draw a rectangle on the image to determine the effective image region;

pic_{i}=imcrop(A{i},[X(1),Y(1),abs(X(1)-X(2)),abs(Y(1)-Y(2))])——Clip the image according to the drawn effective image region;

R{i}=pic_{i}(:,:,1)——Read the R value of the image;

G{i}=pic_{i}(:,:,2)——Read the G value of the image;

B{i}=pic_{i}(:,:,3)——Read the G value of the image;

r{i,1}=mean(R{i})——Average the R value in the X-axis direction;

g{i,1}=mean(G{i})——Average the G value in the X-axis direction;

b{i,1}=mean(B{i})——Average the B value in the X-axis direction;

hsv{i}=rgb2hsv(pic_{i})——Change the image from RGB to HSV;

H{i}=hsv{i}(:,:,1)——Read the H value of the image;

S{i}=hsv{i}(:,:,2)——Read the S value of the image;

V{i}=hsv{i}(:,:,3)——Read the V value of the image;

h{i,1}=mean(H{i})——Average the H value in the X-axis direction;

s{i,1}=mean(S{i})——Average the S value in the X-axis direction;

v{i,1}=mean(V{i})——Average the V value in the X-axis direction;

Gray{i}=rgb2gray(pic_{i})——Convert the image from RGB to gray value;

gray{i,1}=mean(Gray{i})——Average the gray value in the X-axis direction;

end——End the for loop.

Note S3 The content of the configuration file for MyApp.

The initial image taken by the mobile phone is 3000*4000 pixels. The configuration file selects x_{max}, x_{min}, y_{max}, and y_{min} for the spectral region of each channel. For one channel, a rectangular region can be determined by these four points to limit the range of subsequent calculation and value. In addition, based on the rectangular region, x axis is scaled to reduce the calculation error caused by the difference between the two sides and the middle part of the spectral image (**Eq. S2**).

$$(x_1, x_2) = (x_{min} + \frac{x_{max} - x_{min}}{k}, x_{max} - \frac{x_{max} - x_{min}}{k}) \quad \text{(S2)}$$

where x_1 and x_2 are scaled coordinates, k is the scaling factor set according to the specific situation ($k \geq 2$).

(x_1, y_{min}), (x_2, y_{max}), (x_1, y_{min}), (x_2, y_{max}) are the four vertices of the rectangular image region.

Note S4 Reagents and Methods for water quality index analysis.

Reagents:

Phosphoric acid (H_3PO_4 ≥85.0%), concentrated sulfuric acid (H_2SO_4 98%, GR), and potassium cyanide (KCN) were purchased from Sinopharm Chemical Reagent Co., Ltd (Beijing, China). Hydrochloric acid (HCl 36%), sodium hydroxide (NaOH), and acetone (CH_3COCH_3) were purchased from Beijing Chemical Works Co., Ltd (Beijing, China). Sodium nitroprusside {$Na_2[Fe(CN)_5NO]\cdot 2H_2O$}, sodium citrate ($C_6H_5O_7Na_3\cdot 2H_2O$), sodium carbonate ($Na_2CO_3$), sodium bicarbonate ($NaHCO_3$), sodium hypochlorite (NaClO), and stannous chloride ($SnCl_2\cdot 2H_2O$) were purchased from Shanghai Macklin Biochemical Co., Ltd (Shanghai, China). Standard solutions of turbidity, Cr (VI), Fe, and Zn, salicylic acid ($C_6H_4OHCOOH$), ammonium molybdate [$(NH_4)_2MoO_4$], diphenyl carbamide [$OC(HNNHC_6H_5)_2$], 1,10-phenanthroline ($C_{12}H_8N_2$), hydroxylamine hydrochloride ($HONH_2HCl$), ammonium acetate ($NH_4C_2H_3O_2$), ethanoic acid (CH_3COOH, GR), boric acid (H_3BO_3), Zn reagent [$HOC_6H_3(SO_3H)N$: $NC(C_6H_5)$: NNC_6H_4COOH], methanol (CH_3OH), and cyclohexanone ($C_6H_{10}O$) were purchased from Aladdin Bio-Chem Technology Co., Ltd (Shanghai, China).

If not especially specified, the chemicals used in the study were of analytical grade.

Methods:

Turbidity was directly measured at the wavelength of 680 nm.

The salicylic acid method was adopted for colorimetric detection of ammonia nitrogen, which formed blue compound with the maximum absorption wavelength of 655 nm by mixing with sodium salicylate and sodium hypochlorite in alkaline solution.

The phosphorus molybdenum blue method was adopted for colorimetric detection of orthophosphate, which formed blue complex with the maximum absorption wavelength of 650 nm by mixing with ammonium molybdate to form molybdophosphate heteropoly acid and mixing with stannous chloride to reduce molybdophosphate heteropoly acid in acid solution.

The 1,5-diphenylcarbazide method was adopted for colorimetric detection of Cr (VI), which formed amaranth complex with the maximum absorption wavelength of 540 nm by mixing with 1,5-diphenylcarbazide in acid solution.

The 1,10-phenanthroline method was adopted for colorimetric detection of Fe, which formed orange complex with the maximum absorption wavelength of 510 nm by reducing high valance Fe with hydroxylamine hydrochloride and mixing with 1,10-phenanthroline at pH3.0-9.0.

The Zn reagent method was adopted for colorimetric detection of Zn, which formed

blue complex with the maximum absorption wavelength of 620 nm by mixing with Zn reagent at pH9.0.

All the used reagents were of analytical grade and prepared using ultrapure water (Milli-Q, Millipore, 18.2 MΩ/cm) without further purification.

More details can be found in the standard methods for water and wastewater monitoring (The State Environmental Protection Administration, 2002).

Reference

The State Environmental Protection Administration (2002). Water and wastewater monitoring and analysis method (Fourth Edition). China Environmental Science Press: Beijing